

Unified Equations of State for Neutron Stars and Magnetars

OUTER LAYER
1 meter thick
solid or liquid

CORE
10-15 kilometer deep
liquid

Nicolas Chamel

Institute of Astronomy and Astrophysics
Université Libre de Bruxelles, Belgium

Main collaborators: S. Goriely, J. M. Pearson, A. F. Fantina, A. Pastore,
P. Haensel, J.-L. Zdunik, J. Margueron, C. J. Pethick, S. Reddy, D. Page



ULB



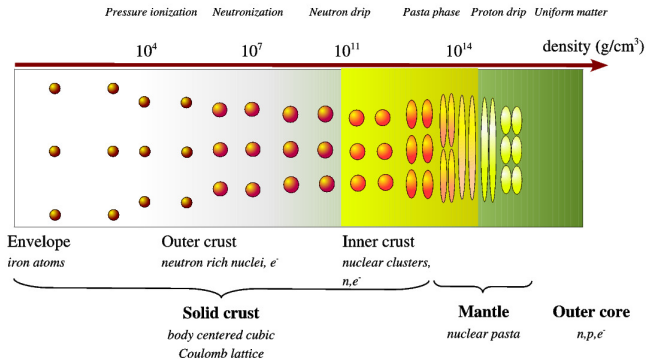
CRUST
1 kilometer thick
solid

RAGtime 16, Prague, October 16, 2014

NEUTRON STAR

Challenge

Neutron star interiors exhibit very different phases of matter:



<http://relativity.livingreviews.org/Articles/lrr-2008-10/>

Our goal is to describe all these phases in a *unified* and *consistent* way using the *same* nuclear model.

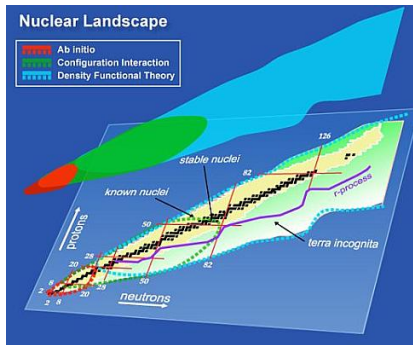
Outline

- 1 Effective nuclear models of dense matter
- 2 Internal constitution of neutron stars/magnetars
- 3 Conclusions & Perspectives

Effective nuclear models of dense matter

Nuclear energy density functional theory in a nut shell

This theory allows for a **tractable and consistent** treatment of atomic nuclei in the outer crust of a neutron star, clusters in the inner crust and nuclear matter in the core.



What is it all about ?

The energy E is a functional of $\rho(\mathbf{r})$, $\tau(\mathbf{r})$ and $\mathbf{J}(\mathbf{r})$, which are built from wavefunctions $\varphi(\mathbf{r})$ obeying $h(\mathbf{r})\varphi(\mathbf{r}) = \varepsilon\varphi(\mathbf{r})$, with

$$h \equiv -\nabla \cdot \frac{\delta E}{\delta \tau} \nabla + \frac{\delta E}{\delta \rho} - i \frac{\delta E}{\delta \mathbf{J}} \cdot \nabla \times \boldsymbol{\sigma} .$$

This scheme can be extended to account for pairing (HFB).

Problem: we don't know what the exact functional is... We have thus to rely on phenomenological functionals.

Which functional should we choose?

A parametrized form of the functional is assumed (e.g. Skyrme), and the free parameters are fitted to some set of nuclear data.

However, most functionals are not suitable for neutron stars:

- they were adjusted to a few selected nuclei (mostly with equal numbers of neutrons and protons)
- they yield unrealistic neutron-matter equation of state
- they yield unrealistic pairing gaps in nuclear matter
- they yield unrealistic effective masses
- they lead to spurious instabilities in nuclear matter (e.g. ferromagnetic transition).

Dense matter equation of state

The diversity of functionals reflects the theoretical uncertainties in the properties of nuclear systems.

In particular, the energy per nucleon of cold nuclear matter can be expanded as

$$e(n, \eta) = e_0(n) + S(n)\eta^2 + o(\eta^4) \text{ where } \eta = (n_n - n_p)/n$$

$$e_0(n) = a_v + \frac{K_v}{18}\epsilon^2 - \frac{K'}{162}\epsilon^3 + o(\epsilon^4) \text{ with } \epsilon = (n - n_0)/n_0$$

$$S(n) = J + \frac{L}{3}\epsilon + \frac{K_{sym}}{18}\epsilon^2 + o(\epsilon^3) \text{ is the symmetry energy.}$$

Note that $S(n) \approx e(n, 1) - e(n, 0)$.

The nuclear parameters (J , L , K_v , etc.) are known with some uncertainties from experiments and microscopic calculations.

Brussels-Montreal Skyrme functionals (BSk)

These functionals were fitted to both experimental data and N-body calculations using realistic forces.

Experimental data:

- all atomic masses with $Z, N \geq 8$ from the Atomic Mass Evaluation (root-mean square deviation: 0.5-0.6 MeV)
<http://www.astro.ulb.ac.be/bruslib/>
- charge radii
- symmetry energy $29 \leq J \leq 33$ MeV
- compressibility $230 \leq K_v \leq 250$ MeV

N-body calculations using realistic forces:

- equation of state of pure neutron matter
- 1S_0 pairing gaps in symmetric and neutron matter
- effective masses in nuclear matter

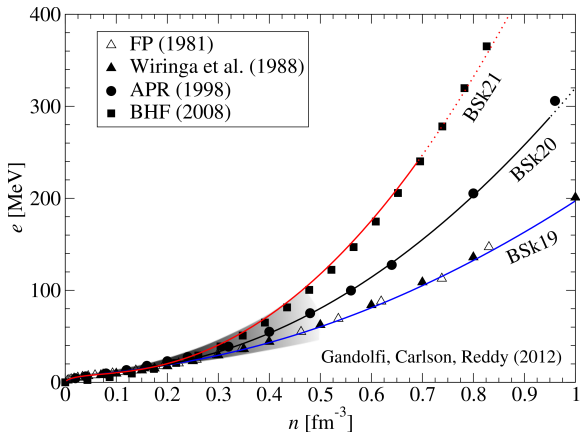
Brussels-Montreal Skyrme functionals

Main features of the latest functionals:

- ▶ **fit to realistic 1S_0 pairing gaps** in symmetric and neutron matter (BSk16-17)
Chamel, Goriely, Pearson, Nucl.Phys.A812,72 (2008)
Goriely, Chamel, Pearson, PRL102,152503 (2009).
- ▶ **removal of spurious spin and spin-isospin instabilities** in nuclear matter (BSk18)
Chamel, Goriely, Pearson, Phys.Rev.C80,065804(2009)
- ▶ **fit to realistic neutron-matter equation of state** (BSk19-21)
Goriely, Chamel, Pearson, Phys.Rev.C82,035804(2010)
- ▶ **fit to different symmetry energies** (BSk22-26)
Goriely, Chamel, Pearson, Phys.Rev.C88,024308(2013)
- ▶ **optimal fit of the 2012 AME** - rms 0.512 MeV (BSk27*)
Goriely, Chamel, Pearson, Phys.Rev.C88,061302(R)(2013)

Neutron-matter equation of state

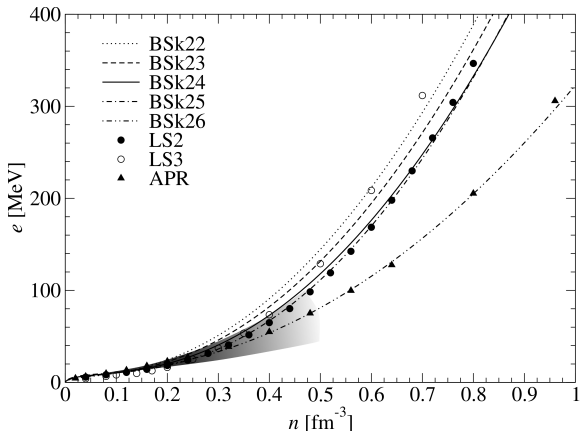
The functionals BSk19, BSk20 and BSk21 were fitted to realistic neutron-matter equations of state with different degrees of stiffness but the same $J = 30$ MeV:



Goriely, Chamel, Pearson, *Phys. Rev. C* 82, 035804 (2010).

Neutron-matter equation of state at high densities

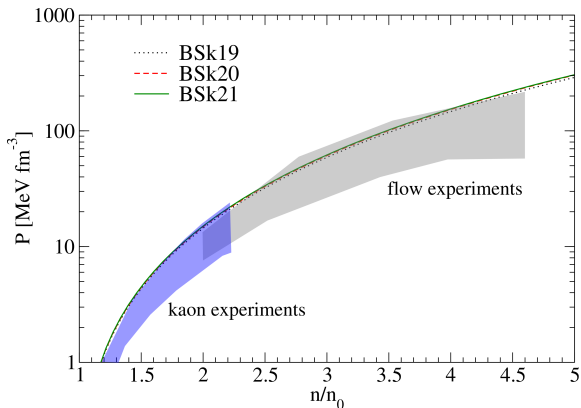
The functionals BSk22-26 were fitted to realistic neutron-matter equations of state with different symmetry energy J :



Goriely, Chamel, Pearson, *Phys.Rev.C* 88, 024308 (2013).

Symmetric nuclear-matter equation of state

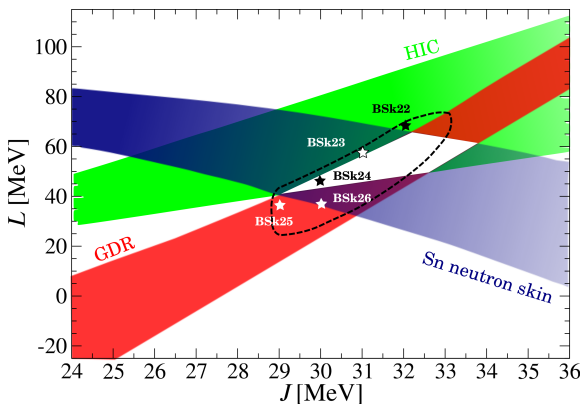
Our functionals are also in good agreement with the constraints obtained from heavy-ion collisions:



Danielewicz et al., Science 298, 1592 (2002); Lynch et al., Prog. Part. Nuc. Phys.62, 427 (2009)

Symmetry energy

The values of J and L obtained from about 30 different HFB atomic mass models (rms < 0.84 MeV) are consistent with other experimental constraints



Internal constitution of neutron stars/magnetars

Description of neutron star crust below neutron drip

Cold catalyzed matter hypothesis

The interior of a neutron is supposed to be in full thermodynamic equilibrium at zero temperature.

Harrison, Thorne, Wakano, Wheeler, Gravitation Theory and Gravitational Collapse (University of Chicago Press, 1965).

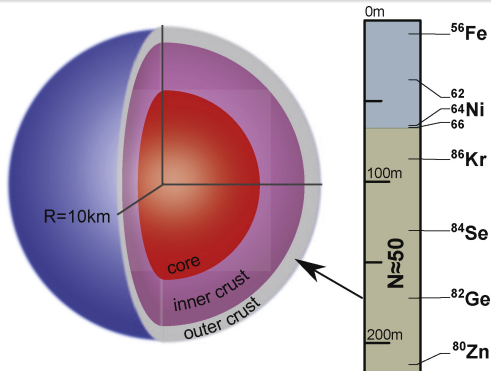
The equilibrium structure of the outer crust of a neutron star for $\rho \gtrsim 10^7 \text{ g cm}^{-3}$ can be determined using the BPS model:

- fully ionized atoms arranged in a perfect (bcc) lattice
- homogeneous crystal at any given pressure
- uniform relativistic electron Fermi gas.

The only microscopic inputs are nuclear masses. We have made use of the experimental data (Atomic Mass Evaluation) complemented with our HFB mass tables.

Composition of the outer crust of a neutron star

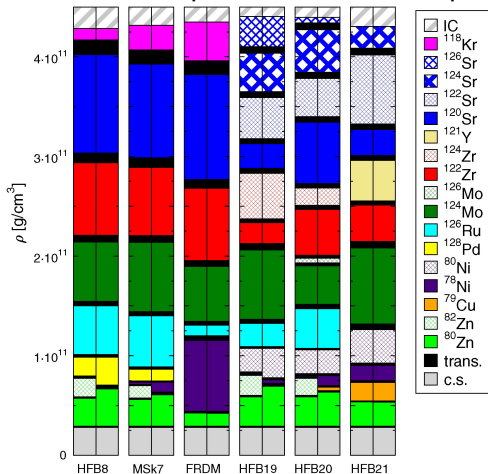
The composition of the crust is completely determined by experimental nuclear masses down to about 200m for a $1.4M_{\odot}$ neutron star with a 10 km radius



Pearson, Goriely, Chamel, Phys. Rev. C83, 065810 (2011); Kreim, Hempel, Lunney, Schaffner-Bielich, Int. J. M. Spec. 349-350, 63 (2013)

Composition of the outer crust of a neutron star

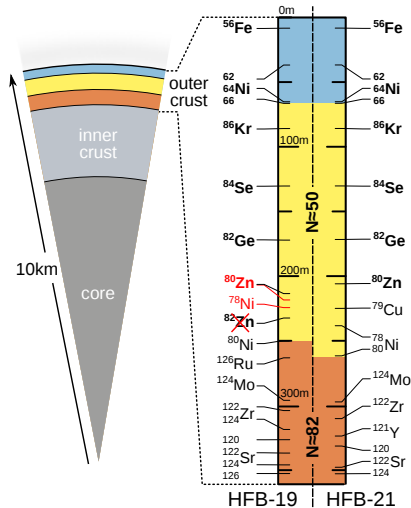
Deeper in the star, the composition is model-dependent:



Pearson, Goriely, Chamel, Phys. Rev. C83, 065810 (2011); Kreim, Hempel, Lunney, Schaffner-Bielich, Int. J. M. Spec. 349-350, 63 (2013)

Plumbing neutron stars to new depths

New precision measurements of the mass of short-lived zinc nuclides by the ISOLTRAP collaboration at CERN's ISOLDE radioactive-beam facility has recently allowed to "drill" deeper into the crust.



Wolf et al., PRL 110, 041101 (2013).

Impact of a strong magnetic field on the composition of the crust?

In a strong magnetic field B (along let's say the z -axis), the **electron motion perpendicular to the field is quantized** into Landau-Rabi levels:



$$e_\nu = \sqrt{c^2 p_z^2 + m_e^2 c^4 (1 + 2\nu B_\star)}$$

where $\nu = 0, 1, \dots$

$$B_\star = B/B_c$$

$$B_c = m_e^2 c^3 / \hbar e \simeq 4.4 \times 10^{13} \text{ G.}$$

Only $\nu = 0$ is filled for $\rho < 2.07 \times 10^6 \left(\frac{A}{Z}\right) B_\star^{3/2} \text{ g cm}^{-3}$.

Landau quantization can impact the composition of the crust.

Composition of the outer crust of a magnetar

Sequence of nuclides for HFB-21 and $B_* \equiv B/(4.4 \times 10^{13} \text{ G})$:

$B_* = 0$	$B_* = 1$	$B_* = 10$	$B_* = 100$	$B_* = 1000$	$B_* = 2000$
⁵⁶ Fe	⁵⁶ Fe	⁵⁶ Fe	⁵⁶ Fe	⁵⁶ Fe	⁵⁶ Fe
⁶² Ni	⁶² Ni	⁶² Ni	⁶² Ni	⁶² Ni	⁶² Ni
⁵⁸ Fe	⁵⁸ Fe	—	—	—	—
⁶⁴ Ni	⁶⁴ Ni	⁶⁴ Ni	⁶⁴ Ni	⁶⁴ Ni	—
⁶⁶ Ni	⁶⁶ Ni	⁶⁶ Ni	—	—	—
—	—	—	—	⁸⁸ Sr	⁸⁸ Sr
⁸⁶ Kr	⁸⁶ Kr	⁸⁶ Kr	⁸⁶ Kr	⁸⁶ Kr	⁸⁶ Kr
⁸⁴ Se	⁸⁴ Se	⁸⁴ Se	⁸⁴ Se	⁸⁴ Se	⁸⁴ Se
⁸² Ge	⁸² Ge	⁸² Ge	⁸² Ge	⁸² Ge	⁸² Ge
—	—	—	—	—	¹³² Sn
⁸⁰ Zn	⁸⁰ Zn	⁸⁰ Zn	⁸⁰ Zn	⁸⁰ Zn	⁸⁰ Zn
—	—	—	—	—	¹³⁰ Cd
—	—	—	—	—	¹²⁸ Pd
—	—	—	—	—	¹²⁶ Ru
⁷⁹ Cu	⁷⁹ Cu	⁷⁹ Cu	⁷⁹ Cu	⁷⁹ Cu	—
⁷⁸ Ni	⁷⁸ Ni	⁷⁸ Ni	⁷⁸ Ni	⁷⁸ Ni	—
⁸⁰ Ni	⁸⁰ Ni	⁸⁰ Ni	⁸⁰ Ni	⁸⁰ Ni	—
¹²⁴ Mo	¹²⁴ Mo	¹²⁴ Mo	¹²⁴ Mo	¹²⁴ Mo	¹²⁴ Mo
¹²² Zr	¹²² Zr	¹²² Zr	¹²² Zr	¹²² Zr	¹²² Zr
¹²¹ Y	¹²¹ Y	¹²¹ Y	¹²¹ Y	¹²¹ Y	¹²¹ Y
¹²⁰ Sr	¹²⁰ Sr	¹²⁰ Sr	¹²⁰ Sr	¹²⁰ Sr	¹²⁰ Sr
¹²² Sr	¹²² Sr	¹²² Sr	¹²² Sr	¹²² Sr	¹²² Sr
¹²⁴ Sr	¹²⁴ Sr	¹²⁴ Sr	¹²⁴ Sr	¹²⁴ Sr	¹²⁴ Sr

Composition of the outer crust of a magnetar

Sequence of equilibrium nuclides with increasing depth in the outer crust of a magnetar for two different HFB atomic mass models and $B_{\star} = 2000$.

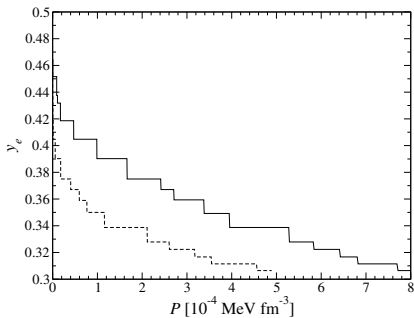
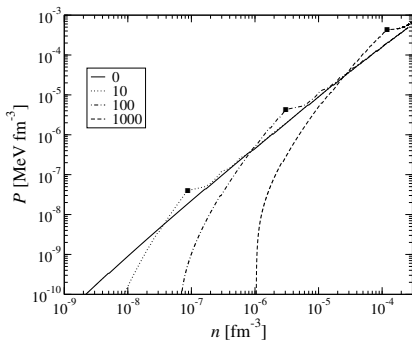
HFB-24	HFB-27*
^{56}Fe (3.12×10^{-7})	^{56}Fe (3.12×10^{-7})
^{62}Ni (1.23×10^{-5})	^{62}Ni (1.23×10^{-5})
^{88}Sr (2.68×10^{-5})	^{88}Sr (2.68×10^{-5})
^{86}Kr (7.06×10^{-5})	^{86}Kr (7.06×10^{-5})
^{84}Se (1.46×10^{-4})	^{84}Se (1.46×10^{-4})
^{82}Ge (2.44×10^{-4})	^{82}Ge (2.44×10^{-4})
^{132}Sn (2.56×10^{-4})	^{132}Sn (2.56×10^{-4})
^{80}Zn (3.31×10^{-4})	^{80}Zn (3.31×10^{-4})
^{130}Cd (3.69×10^{-4})	^{130}Cd (3.85×10^{-4})
^{128}Pd (4.98×10^{-4})	^{128}Pd (5.07×10^{-4})
^{126}Ru (5.78×10^{-4})	^{126}Ru (5.81×10^{-4})
^{124}Mo (7.72×10^{-4})	^{124}Mo (7.99×10^{-4})
^{122}Zr (8.83×10^{-4})	^{122}Zr (8.94×10^{-4})
^{121}Y (8.98×10^{-4})	—
—	^{124}Zr (9.72×10^{-4})
^{120}Sr (9.82×10^{-4})	^{120}Sr (9.83×10^{-4})
^{122}Sr (1.11×10^{-3})	^{122}Sr (1.15×10^{-3})
^{124}Sr (1.15×10^{-3})	—

The nuclides with experimentally measured masses are indicated in boldface. The maximum pressure at which each nuclide can be found is indicated in parenthesis in units of MeV fm^{-3} .

Chamel et al., Bulg. J. Phys. 40, 275 (2013).

Equation of state of the outer crust of magnetars

Matter in a magnetar is much more incompressible and less neutron-rich than in a neutron star.

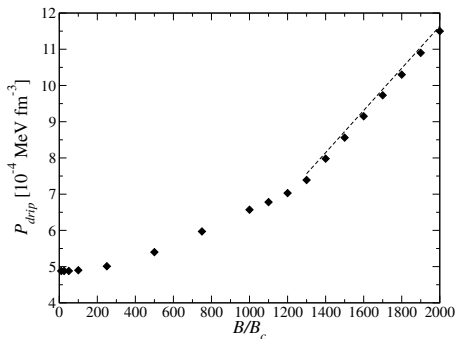


$$P \approx P_0 \left(\frac{n}{n_s} - 1 \right)^2$$

$$y_e \approx \frac{1}{2} \left(1 - \sqrt{\frac{\pi^2 \lambda_e^3 m_e c^2 P}{4 B_* J^2}} \right)$$

Neutron drip transition in magnetars

The neutron drip pressure is found to increase with B whereas the composition of matter remains the same:



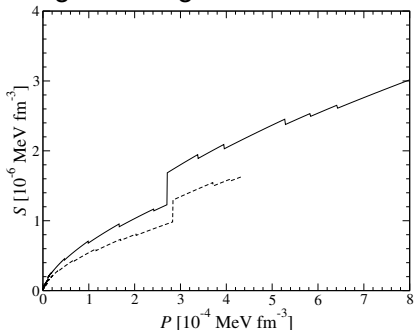
In the strongly quantizing regime, $P_{\text{drip}} = \frac{m_e c^2}{\lambda_e^3} \frac{(\gamma_e^{\text{drip}})^2}{4\pi^2} B_\star$

Chamel et al., Phys.Rev.C86, 055804(2012).

Transport properties in magnetars

Strongly quantizing magnetic fields can impact transport properties

e.g. the magnetic field increases the shear modulus:



$S = 0.1194 n_N \frac{Z^2 e^2}{R_N}$ where R_N
is the ion-sphere radius

$$R_N = \left(\frac{3}{4\pi n_N} \right)^{1/3}$$

solid line: $B_\star = 1400$

dashed line: $B_\star = 0$

Chamel et al., Phys.Rev.C86, 055804(2012).

Description of neutron star crust beyond neutron drip

We have determined the equilibrium structure of the inner crust of a neutron star for $\rho \gtrsim 4 \times 10^{11} \text{ g cm}^{-3}$ using the Extended Thomas-Fermi+Strutinsky Integral method (ETFSI):

- spherical neutron-proton clusters coexisting with a neutron liquid using parametrized density distributions (Wigner-Seitz approximation for the Coulomb energy),
- proton shell effects added perturbatively,
- uniform relativistic electron gas.

Pearson,Chamel,Goriely,Ducoin,Phys.Rev.C85,065803(2012).

Advantages of ETFSI method

- very fast approximation to the full Hartree-Fock method
- avoids the difficulties related to boundary conditions

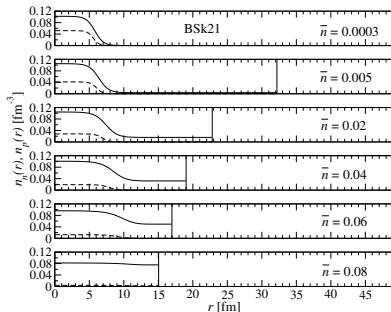
Chamel et al.,Phys.Rev.C75(2007),055806.

Structure of the inner crust of a neutron star (I) nucleon distributions

With increasing density, the clusters keep essentially the same size but become more and more dilute:

Crust-core transition properties

	\bar{n}_{cc} (fm^{-3})	P_{cc} (MeV fm^{-3})
BSk19	0.0885	0.428
BSk20	0.0854	0.365
BSk21	0.0809	0.268
SLy4	0.0798	0.361



Open issues: pastas?

The crust dissolves almost continuously into a uniform mixture of nucleons and electrons.

Structure of the inner crust of a neutron star (II) composition

With SLy4, BSk19, BSk20 and BSk21, only $Z = 40$ is found.

Comparison of inner- and outer-crust codes at drip point; results for latter code in parentheses. e is the internal energy per nucleon, and P the pressure.

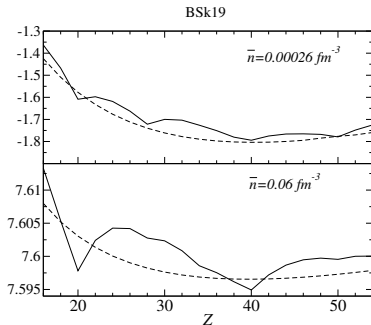
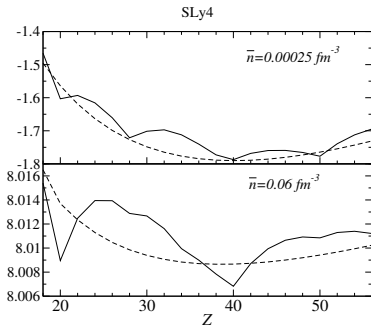
	$\bar{n}_{\text{drip}} \text{ (fm}^{-3}\text{)}$	Z	N	$e \text{ (MeV)}$	$P \text{ (} 10^{-4} \text{ MeV fm}^{-3}\text{)}$
BSk19	2.63×10^{-4}	40 (38)	96 (88)	-1.79 (-1.87)	5.1 (4.9)
BSk20	2.63×10^{-4}	40 (38)	95 (88)	-1.79 (-1.87)	5.1 (4.9)
BSk21	2.57×10^{-4}	40 (38)	94 (86)	-1.82 (-1.90)	5.0 (4.9)
SLy4	2.46×10^{-4}	40 (38)	93 (82)	-1.79 (-1.96)	4.7 (4.8)

The few % discrepancies can be attributed to

- the neglect of pairing,
- the neglect of neutron shell effects,
- the parametrized density distributions,
- the neglect of rotational and vibrational corrections.

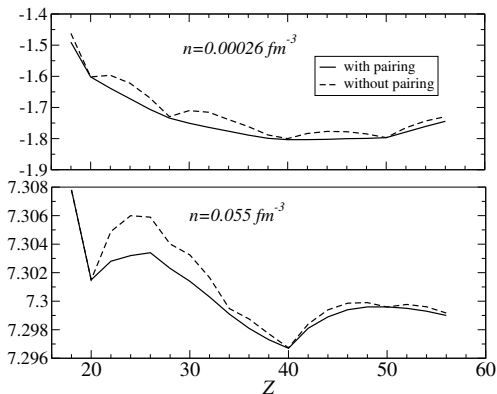
Structure of the inner crust of a neutron star (II)

- The ordinary nuclear shell structure seems to be preserved apart from $Z = 40$ (quenched spin-orbit?).
- The energy differences between different configurations become very small as the density increases!



Structure of the inner crust of a neutron star (III) composition

Impact of proton pairing (BCS approximation) with BSk21



Impact of neutron pairing
on the crust structure?

Pearson,Chamel,Pastore,Goriely,submitted.

In a real neutron star, a large range of values of Z is expected.

Unified equations of state of neutron stars

The same functionals used in the crust can be also used in the core (n, p, e^-, μ^-) thus providing a **unified and thermodynamically consistent description of neutron stars**.

Tables of the full equations of state:

[http:](http://vizier.cfa.harvard.edu/viz-bin/VizieR?-source=J/A+A/559/A128)

[//vizier.cfa.harvard.edu/viz-bin/VizieR?-source=J/A+A/559/A128](http://vizier.cfa.harvard.edu/viz-bin/VizieR?-source=J/A+A/559/A128)

Fantina, Chamel, Pearson, Goriely, A&A 559, A128 (2013)

Analytical representations of the full equations of state:

<http://www.ioffe.ru/astro/NSG/BSk/>

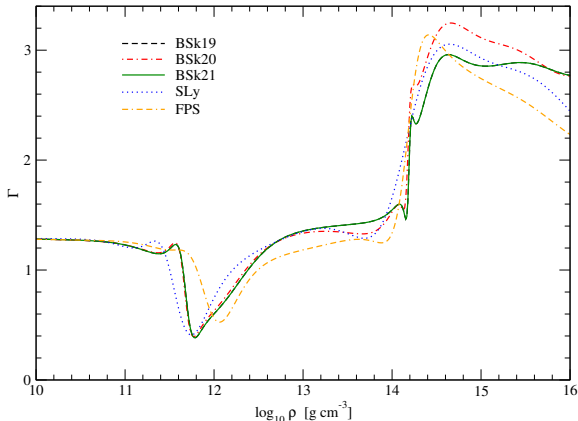
Potekhin, Fantina, Chamel, Pearson, Goriely, A&A 560, A48 (2013)

EoSs for the latest BSk functionals will appear soon.

Pearson, Chamel, Fantina, Goriely, Eur. Phys. J. A 50, 43 (2014)

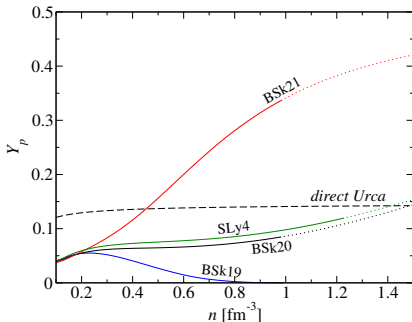
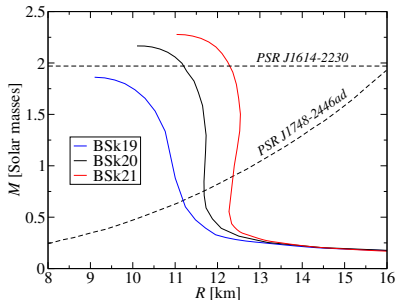
Adiabatic index of neutron-star matter

Realistic equations of state of neutron stars can hardly be parametrized by polytropes:



Neutron star structure

With these unified equations of state, we have computed the global structure of neutron stars by solving the TOV equations.

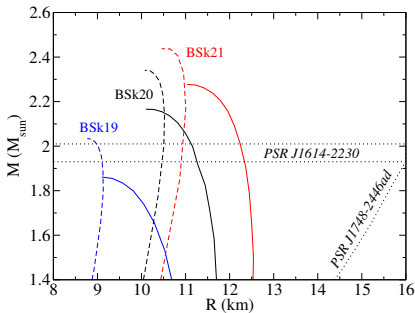


The proton fraction Y_p is mainly determined by the symmetry energy: $\mu_e(n) Y_p^{1/3} \approx 4S(n)(1 - 2Y_p)$.

Chamel, Fantina, Pearson, Goriely, Phys.Rev.C84,062802(R)(2011).

Unified equation of state of hybrid stars

Observations do not necessarily rule out the BSk19 functional.



Assuming a phase transition occurs at a baryon density above 0.2 fm^{-3} provided it lowers the Gibbs free energy for a given pressure:

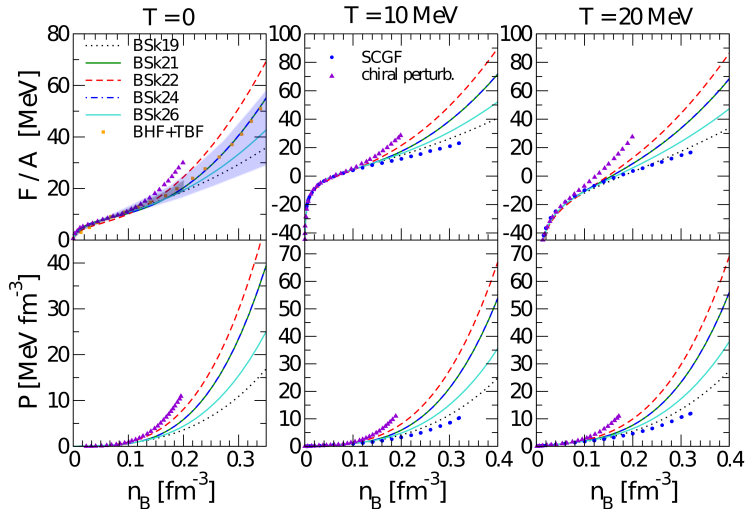
	$\mathcal{M}_{max}/M_{\odot}$
BSk19	2.03
BSk20	2.31
BSk21	2.42

Massive neutron stars could still be compatible with the BSk19 functional if their core contains “exotic” matter with a stiff enough equation of state.

Chamel et al., A&A 553, A22 (2013)

Equation of state of hot dense matter

We have also begun to extend our EoS for supernova cores.



Conclusions & Perspectives

OUTER LAYER
1 meter thick
solid or liquid

CORE
10-15 kilometer deep
liquid

We have developed unified equations of state of cold dense nucleonic matter for nonaccreting neutron stars and magnetars.

Tables:

[http:](http://vizier.cfa.harvard.edu/viz-bin/VizieR?-source=J/A+A/559/A128)

[//vizier.cfa.harvard.edu/viz-bin/VizieR?-source=J/A+A/559/A128](http://vizier.cfa.harvard.edu/viz-bin/VizieR?-source=J/A+A/559/A128)

Fantina, Chamel, Pearson, Goriely, A&A 559, A128 (2013)

Analytical representations (fortran subroutines):

<http://www.ioffe.ru/astro/NSG/BSk/>

Potekhin, Fantina, Chamel, Pearson, Goriely, A&A 560, A48 (2013)

Perspectives: hot dense matter in accreting neutron stars, proto-neutron stars and supernova cores.

CRUST
1 kilometer thick
solid